RESEARCH Open Access

Enhanced porcine gut barrier functioning and reduced inflammation from a combination of seaweed bioactives

Meike A. Bouwhuis¹, Irene H. G. Nooijen², Evita van de Steeg² and Shane O'Connell^{1,3*}

Abstract

Background Microbial and toxin-related challenges are well-documented causes of impaired animal performance. The gastro-intestinal tract is the single largest organ that interfaces with numerous challenges including pathogenic organisms, toxins and other immune activating stimuli. The integrity of the intestinal mucosal barrier is the first and most critical line of defence. There are a number of reports demonstrating the potential of naturally derived feed additives to mitigate the damage derived from toxin or infectious agents on cell culture barrier integrity models but little information on target species tissue. Natural ingredients based on *Lithothamnion glaciale* (LG) and an extract of *Ascophyllum nodosum* (ANE) were tested in an ex vivo model using porcine ileal tissue, in the absence and presence of an infectious challenge derived from *Salmonella enterica enteriditis* (SEE). Read-outs included various parameters on the barrier integrity, tissue histology as well as the immune status of the tissue.

Results The SEE challenge significantly impaired barrier integrity (P<0.05), as demonstrated by increased paracellular ([3H]-mannitol) relative to transcellular ([14C]-caffeine) transport. LG and ANE were tested individually at multiple doses and in combination to explore potential synergistic effects. The barrier integrity was positively impacted from the combination of LG and ANE at the low ANE dose, especially following the SEE challenge (P<0.001). The SEE challenge reduced TNF- α expression in the control treatment, which is caused by the downregulation of the inflammatory response immediately after a challenge (P<0.01). The relative expression of the gut barrier protein Cadherin-17 was increased when LG and/or ANE was included (P<0.001), both with and without the SEE challenge. The inflammatory markers tumour necrosis factor- α , Caspase-1, Interleukin-22 and regenerating islet-derived protein-3 γ were affected by the inclusion of LG and/or ANE (P<0.05). A synergistic effect between the two marine bioactives was evident and appears to be dose dependent, with the low dose rate of ANE and the low and medium LG rate being most optimal.

Conclusions These results suggest that an optimal combination of marine bioactives can have a significant effect in enhancing gut barrier integrity and immune reactivity when challenged with an intestinal pathogenic bacteria in porcine ileal tissue.

Keywords Marine bioactives, *Ascophyllum nodosum*, *Lithothamnion sp.*, Gut barrier, Gut integrity, Salmonella infection, Piglet health

*Correspondence: Shane O'Connell shane.oconnell@marigot.ie Full list of author information is available at the end of the article



Background

A strong, healthy gut barrier is of vital importance for pigs and all other animal species. A disrupted gut barrier means that it is easier for pathogens and toxins to enter the blood stream and cause systemic inflammation, tissue damage and subsequent losses in production [1, 2]. Vital for a healthy gut barrier is the presence of tight junction proteins, which connect epithelial cells and close off the space between cells to prevent uncontrolled permeability [1]. Different stressors can be held accountable for the reduction in gut barrier strength, depending on age, physiological status and the environment of the animals. In newly weaned piglets, gut barrier issues are well recognized and described [1, 3]. Due to the practices surrounding weaning such as removal from the sow, change-over in diet and unfamiliar housing, piglets experience stress and subsequently reduce their feed intake for a period. This has significant implications on the structure and function of the gastro-intestinal tract (GIT), causing inflammation, impaired barrier function and increasing gut permeability [3, 4]. In addition, exposure to pathogenic bacterial infection in the GIT can have a significant impact on barrier integrity leading to overall health and growth performance impairment.

However, intestinal barrier issues are less recognized in breeding sows. Due to physiological stress that sows experience around and immediately after farrowing, it can be suggested that these pigs also suffer from increased gut permeability. Secondly, farrowing room temperatures are set to accommodate the sow, while the higher temperature requirement of the piglet is accommodated by heat lamps or heat pads. However, the actual room temperature will still be above the comfort temperature of the sow [5, 6] causing heat stress for the dam. Heat stress is a known factor for causing intestinal inflammation and increased gut permeability [7] and this could therefore impact sow gut health and productivity.

To enhance pig health and performance, many different feed additives and ingredients have been researched to enhance the gut barrier, especially in weaned piglets [2, 4]. Two potential marine bioactive ingredients that have been demonstrated to enhance the gut barrier are Lithothamnion glaciale (LG) and an extract from the brown seaweed Ascophyllum nodosum (ANE). LG is a calcified seaweed that grows around the coast of Iceland and contains 3%w/w organic material, 95% inorganic material including 30% calcium, 3% magnesium and 72 other trace minerals. Several studies have demonstrated that LG supports gut barrier integrity and reduces intestinal permeability in both in vitro and human studies [8-10]. Aslam et al. [10] reported that LG supplementation increased the thickness of the protective mucous layer on top of the epithelial cells and increased the protein expression of cadherins and laminins. These proteins are key for the formation of the tight junctions and basement membrane. A subsequent study by the same group [9] found that the presence of LG increased the number of desmosomes, further indicating its role in strengthening epithelial cell-cell adhesion and overall barrier function.

ANE contains high levels of the β-glucan, laminarin and the sulphated polysaccharide fucoidan. These structures are difficult to digest enzymatically and are therefore assumed to be fermented in the large intestine [11]. Laminarin and fucoidan from different brown seaweeds have been shown to have anti-inflammatory and immunomodulatory properties through reducing the activation of the NF-κβ pathway and Myd88 response, by interacting with pattern recognition receptors such as Toll-like receptor 4 and reducing the production of proinflammatory cytokines [12-15]. Low-molecular-weight fucoidan has also been shown to enhance IL-10 and IFN-γ production while suppressing IL-1 β and TNF- α in intestinal epithelial models, supporting mucosal immune homeostasis [14]. Additionally, laminarin and fucoidan supplementation in vivo reduced Salmonella Typhimurium colonization and intestinal inflammation in pigs, along with downregulation of IL-6, IL-22, TNF-α, and Reg3γ expression in colonic tissue [15].

In this research, an ex vivo model (InTESTineTM; [16, 17]) utilising porcine ileal tissue was used. The objective of the study was to assess the effect of the LG and ANE bioactives and their combinations on the inflammatory response and gut barrier functioning, in the absence and presence of a pathogenic bacterial strain. It was hypothesized that both LG and ANE would reduce the inflammatory response and reduce gut permeability, with a synergistic effect between LG and ANE.

Methods

Compound selection and characterisation

The Ascophyllum Nodosum extract was provided by Brandon Bioscience (Tralee, co. Kerry, Ireland) and Lithothamnion glaciale was provided by Celtic Sea Minerals (Currabinny, co. Cork, Ireland). The Ascophyllum Nodosum extract was produced using a proprietary processing technology of Brandon Bioscience. Analysis of the compounds was performed as described by Quille et al. [18] for the LG and Goñi et al. [19] for the ANE. These results are presented in Table 1. Briefly, the following analysis was performed. Total solids from ANE were determined after drying in a convection oven for 18 hours at 105 °C. The inorganic and organic composition was determined by heating 3 g of material in triplicate in a furnace at 450 oC for 5 h. Samples were placed in a desiccator to cool overnight and were subsequently weighed. The percentage inorganic matter was calculated by dividing the ash weight

Table 1 Composition of the two test substances *Lithamnion glaciale* and *Ascophyllum Nodosum* extract

Parameter	Lithothamnion glaciale (%w/w)	Ascophyllum Nodosum extract (%w/w)		
Moisture	0.1±0.01	6.5±1.50		
Inorganic material	96.6±0.03	22.8±0.12		
Calcium	29.5±0.20	1.2±0.30		
Magnesium	5.7±0.15	1.2±0.30		
Organic	3.4±0.03	70.7±0.12		
Alginate	ND	13.9±2.34		
Fucoidan	ND	12.5±0.63		
Laminarin	ND	4.2±1.08		
Mannitol	ND	6.9±0.99		
Polyphenol	ND	7.8±0.80		
Other Organic	3.4±0.03	25.4±3.67		

ND Not detected

by the starting weight of the material and multiplying by 100. The organic matter was calculated by the difference between the material weight and the ash weight. The calcium and magnesium composition was determined by first digesting 200 mg of the carbonate materials in 10 mL of nitric acid (65%) in a microwave digester (Mars 6, 240/50 CEM Microwave Technology (Ireland) Ltd., Dublin, Ireland) ramped to 190 oC over 20 min, held at 190 oC for 15 min, cooled for 20 min to 70-80 oC and subsequently analysed using a suitable dilution on an Agilent ICP-MS 7800 instrument (Agilent Technologies Ireland Ltd., Cork, Ireland) tuned using Agilent Tuning Solution for ICP-MS (1 ppb), part No. 5185-5959, and calibrated with Agilent Environmental Calibration Standard, part No. 5183–4688. All ICP-MS elemental calibration curves had r-squared values >0.95.

Sulphate content linked to carbohydrate molecules was determined quantitatively after hydrolysing the samples with 2 M trifluoroacetic acid (TFA) for 5 h at 100 °C. Sulphate ion was precipitated in a strongly acid medium with barium chloride-gelatine. The resulting turbidity was measured spectrophotometrically at 420 nm and compared with an appropriate calibration standard curve using Na2SO4 (0–10 mM). L-fucose, total uronic acids, laminarin and total polyphenol content were determined spectrophotometrically [19]. A quantitative analysis of soluble mannitol from ANEs was carried out by high performance anion exchange chromatography with pulsed amperometric detection (HPAEC15 PAD).

Compound preparation

Based on the feeding rates of the *Ascophyllum Nodosum* extract and *Lithothamnion glaciale* in animal diets, dose

rates were calculated for the InTESTineTM model. The animal feeding rates and InTESTineTM dose rates were calculated based on multiple studies [15, 20–22]. A 3 x 3 factorial design was prepared, with 3 levels of *Lithothamnion glaciale* (37.8 μ g, 63.2 μ g and 88.7 μ g per well) and 3 levels of *Ascophyllum nodosum* extract (2.3 μ g, 4.5 μ g and 9.1 μ g). In addition to the standard control with 2 mM calcium, the high calcium level of *Lithothamnion glaciale* also warranted inclusion of 2 extra calcium control levels, at 3.8 mM and 5.3 mM, respectively. This was to ensure that potential effects were controlled for calcium levels. Lastly, the individual effects of *Lithothamnion glaciale* and *Ascophyllum nodosum* were also investigated.

As the InTESTineTM system utilises small intestinal tissue, a pre-digestion step was included for the *Lithothamnion glaciale* to better mimic the material that would appear in the small intestine. In short, 8.33 g *Lithothamnion glaciale* was diluted in 5 L de-ionized $\rm H_2O$. Subsequently, the diluted sample was titrated with 0.1 M HCl until a pH of 3.5 was reached. Afterwards, the sample was concentrated and dried. Based on its solubility, it was assumed that the *Ascophyllum nodosum* extract would be bioaccessible in the digestive tract, so no pre-digestion step was performed.

Medium and assay buffer preparation

Williams E medium needed for transportation and handling of the intestinal tissue was prepared. Williams E medium was supplemented with D-Glucose (2.75 mg/mL), Glutamax 1% (v/v), Fungizone (2.5 μ g/mL), Gentamicin (50 μ g/mL), HEPES (10 mM) and Penicillin/Streptomycin (P/S) 1% (v/v) (hereafter referred to as Williams E).

The calcium levels of the different test substances were considered during preparation of the different treatments. This resulted in the preparation of 2 extra control formulations where different amounts of calcium were included to control for the calcium levels of the test formulation incubations. In total, 14 different test formulations were applied in the InTESTineTM system as are presented in Table 2. Krebs-Ringer Bicarbonate (KRB) buffer was used as assay buffer. For the preparation of the stock- and dose solutions of the test formulations as well as for the (reference) control incubations, (standard) KRB buffer was used, however, the buffer was prepared with different concentrations of calcium (added in the form of CaCl₂), namely 5.3, 3.8 and 2.0 mM. Also, calcium-free KRB was prepared in which CaCl2 was replaced by KCl. In addition, KRB + 1% Bovine serum albumin (BSA) and KRB + 4% BSA were also prepared.

[14C] Caffeine (1kBq/ml) and [3H] mannitol (10 kBq/ml), used as reference substances for absorption testing, were purchased from Perkin Elmer Inc. (Boston,

Table 2 Description of the test formulations, applicable inclusion rates and calcium levels

Test formulation #	Description	Lithothamnion glaciale inclusion μg/well	Ascophyllum Nodosum inclusion μg/well	Final concentration Ca mM ^a
1	Control – 2.0 mM Ca	-	-	2.0
2	Control – 3.8 mM Ca	-	-	3.8
3	Control – 5.3 mM Ca	-	-	5.3
4	LG 63.2	63.2	-	3.8
5	ANE 2.3	-	2.3	2.3
6	LG 37.8/ANE 2.3	37.8	2.3	2.3
7	LG 37.8/ANE 4.5	37.8	4.5	2.3
8	LG 37.8/ANE 9.1	37.8	9.1	3.8
9	LG 63.2/ANE 2.3	63.2	2.3	3.8
10	LG 63.2/ANE 4.5	63.2	4.5	3.8
11	LG 63.2/ANE 9.1	63.2	9.1	5.3
12	LG 88.7/ANE 2.3	88.7	2.3	5.3
13	LG 88.7/ANE 4.5	88.7	4.5	5.3
14	LG 88.7/ANE 9.1	88.7	9.1	5.3

^a Final concentration Ca based on all calcium present, derived from *Lithothamnion* source and assay buffer. *LG* Lithothamnion glaciale; *ANE* Ascophyllum Nodosum extract.

Massachusetts, United States). All other chemicals were purchased from Sigma- Aldrich Chemie B.V. (Zwijndrecht, the Netherlands). Mannitol and caffeine were used as reference markers for paracellular (low permeability) and transcellular (high permeability) transport, respectively, by measuring the apparent permeability (P_{app}) (ratio) of mannitol and caffeine in the reference compound incubations. The combination of both compounds and therefore the P_{app} ratio was determined only in this reference incubation (n=4), however, mannitol transport was determined in each incubation to monitor paracellular tissue permeability in all test conditions. The integrity of the intestinal tissue was also determined in all test conditions by co-incubation of the dose solutions with FD4 (50 μM). FD4 was measured in the basolateral compartment over time. Furthermore, the tissue viability was determined in all test conditions as well, by measuring the LDH leakage from the tissue into the apical and basolateral compartment. Samples for all described control parameters were collected at t=1, t=2, t=4 and t=5 h.

Addition of Salmonella enterica enteriditis

The 14 test formulations were incubated with the intestinal tissue alone or in co-incubation with the pathogenic bacterial strain *Salmonella enterica enteritidis*. For this, *Salmonella enterica enteritidis* (SEE) was precultured on generic growth medium and on the day of the InTES-Tine experiment, a 10-fold stock concentration of $\sim 1x10^9$ CFU/mL in assay buffer KRB was prepared. From all 14

dose solutions, a sub-portion was taken to which the SEE stock solution was added to obtain $\sim 1 \times 10^8$ CFU/mL for administration in the InTESTine TM system at t=0.

Permeability studies with porcine intestinal tissue

The experiment using porcine intestinal tissue was performed as described in Westerhout et al. [16, 23] and Stevens et al. [17]. Briefly, intestine of a domestic pig (Sus scrofa domesticus) with a body weight of approximately 20 kg was excised. The tissue was washed with ice-cold Williams E + 1% P/S on site and transported to the lab submerged in ice-cold Williams E + 1% P/S. The tissue was immediately used for the ex vivo preparation. The serosa and the muscle layer of the intestinal tissue were carefully removed, continuously submerged under icecold Williams E + 1% P/S during further preparation. Subsequently, the required number of segments with a surface area of 0.246 cm² of ileum tissue was punched out and mounted into the InTESTineTM system with the mucosal side facing upwards. The tissue containing inserts were placed in the plates pre-filled with 875 µL ice-cold KRB and 125 µL of ice-cold KRB was immediately added to the apical compartment. The assembled system was placed in a high oxygen incubator, on a rocker platform (200 rpm) at \sim 37 °C for 30 ± 2 minutes, to allow for slow acclimatization of the tissue to these conditions.

After 30 ± 2 minutes of acclimatization time, the excess formed mucus was carefully removed by resuspension and subsequently discarded. The tissue containing inserts were transferred to the plates pre-filled with warm KRB

+ 4% BSA. Next, the pre-warmed dosing solutions (~37 °C) containing mannitol (10 μM) and caffeine (10 μM) (mixture of non-radiolabelled mannitol and caffeine and [3H]-mannitol and [14C]-caffeine, also referred to as C/M), in addition of FITC dextran 4 (FD4; 50 μM), were applied to the apical compartment, together with the 34 different test solutions and the time point was set as t=0 (all incubations n=4). The apical compartment contained 125 μL dosing solution (in KRB) and the basolateral compartment contained 875 μL KRB + 4% BSA.

At t=0, 25 μL sample aliquots (dose solutions) were taken from the apical side of the reference compound incubations (C/M) for radioactive analysis and 25 μL sample aliquots (dose solutions) were taken from the apical side of the test formulation incubations for radioactive analysis of [3H]-mannitol.

At t=1, t=2, t=4 and t=5 h, sample aliquots of 650 μ L were collected from the basolateral compartment (500 μ L for radioactive analysis, 100 μ L for FD4 and 50 μ L for LDH analyses) and sample aliquots of 65 μ L were taken from the apical compartment (40 μ L for radioactive analysis and 25 μ L for LDH analysis). After sampling at t=1 h, t=2 h and t=4 h, volumes were restored to 125 μ L apical and 875 μ L basolateral by replenishing the compartments with apical dose and basolateral assay buffer, respectively.

After 5 hours of incubation, the intestinal tissue segments of the test formulation incubations (with and without SEE) were harvested by dismounting them from the InTESTineTM system and immediately split in half. The segments for RNA isolation (n=4/condition) were collected in vials (dry, without any medium or buffer) and immediately placed in liquid nitrogen (snap-frozen) followed by storage at \leq -70 °C until further use. The segments for H&E staining (n=4/condition) were collected in histological cassettes and immediately placed in formalin until further use.

Due to mechanical damage to the tissue, histological analysis of the first experiment was not possible. Therefore, the experiment was repeated with the 2.0 mM KRB control and the treatments 6 and 9, LG + AN 1 and LG + AN 4, respectively in the exact same manner as the first, overall experiment. For this second experiment, no RNA extractions were performed.

Tissue permeability, integrity and viability

Aliquots of the radiolabelled study samples ([³H]-mannitol and [¹⁴C]-caffeine) were collected in scintillation vials. After addition of liquid scintillant (Ultima GoldTM) to the vials, the radioactivity was measured by liquid scintillation counting (LSC) on a Tri-Carb 3100 TR liquid scintillation counter using QuantaSmartTM software. All counts were converted to disintegrations per minute (DPM) using tSIE/AEC (transformed Spectral

Index of external standards coupled to Automatic Efficiency Correction). Background values were measured with each sample sequence using scintillant without any sample. Apical to basolateral permeability of the large fluorescent molecule FD4 (MW ~4000) was used as an intestinal tissue integrity marker in all incubations. Samples from the basolateral compartments containing FD4 were analysed using a multi-mode fluorescence spectrometer (Synergy HT, BioTek) at excitation and emission wavelengths of 485 and 528 nm, respectively. The cut-off value typically applied to this parameter is ≤1% FD4 permeability per hour. Lactate dehydrogenase (LDH) leakage from the intestinal tissue into both the apical and basolateral compartment was used as a tissue viability (cell toxicity) marker in all incubations. Total LDH levels in the intestinal segments were determined by homogenizing two control tissue segments (non-exposed tissue) in ice-cold KRB using a tissue dissociator (gentleMACSTM, Miltenyi Biotec). LDH activity in homogenized tissue from control segments (t=-30), as well as in study samples were determined using a LDH kit (Roche Life Science). The cut-off value typically applied to this parameter is ≤3% LDH leakage per hour (apical + basolateral), expressed as cumulative LDH leakage throughout the experiment.

RNA extraction, complementary DNA synthesis and quantitative real-time PCR

RNA isolation from the stored tissue segments was performed using the RNeasy mini kit (Qiagen, Venlo, the Netherlands) following the manufacturer's instructions. A maximum of 30 mg tissue was used. In short, lysis buffer was added to the frozen samples and after thawing, the tissue was disrupted and homogenized. Next, the samples were centrifugated and the supernatant was transferred to columns placed in collection tubes and again centrifugated. After several washing steps, the columns were transferred to new collection tubes and the RNA was eluted from the columns. RNA concentration, purity, and integrity were measured using Qubit (Thermo Fisher Scientific, Waltham, MA, USA). Expression analysis of the genes Desmoglein 2 (DSG2), tumour necrosis factor alpha (TNFα), interleukin 17 receptor A (IL17RA), E-cadherin 17 (CDH17), Caspase-1, Interleukin 22 (IL-22) and regenerating islet-derived protein-3 γ (Reg3-γ) was performed by RT-qPCR using a Roche LightCycler® 96 System (Roche, UK) and a one-step LightCycler® RNA Master SYBR Green I kit (Roche, UK) according to the manufacturer's instructions. The relative expression level of the aforementioned genes was calculated relative to reference genes b2-microglobulin (B2M), glyceraldehyde-3-phosphate dehydrogenase (GAPDH), and peptidylprolyl isomerase A (PPIA), from which GAPDH was the most stable. The $2^{-\Delta\Delta CT}$ method was used to quantify relative normalized gene expression levels. The primerssequences used are shown in Table 3.

Histological analysis

The formalin-fixed Intestinal tissue slices were prepared using standard paraffin embedding techniques (n=2/condition). Hereafter, haematoxylin and eosin staining was performed on the slices and pictures were taken. The pictures from the histological samples were assessed by a pathologist.

Calculations and statistical analysis

The apparent permeability values (P_{app} values, cm/s) representing the apical (mucosal) to basolateral (serosal) permeability of caffeine and mannitol was calculated between 1–2 hours, 2–4 hours and 4–5 hours using the following equation: $P_{app} = \frac{dQ/dt}{SA \times C_{Api,0}}$. Here, dQ/dt indicated the appearance rate of the compound at the basolateral side over time, SA is the surface area of the exposed tissue and Capi,0 is the initial dose concentration of the compound. The acceptance criterion for this parameter is a Papp ratio (P_{app} caffeine/ P_{app} mannitol) ≥ 2 for porcine ileum tissue under control conditions. The leakage of FD4 into the basolateral compartment was calculated as percentage of dose using the following equation: $4leakage = \frac{rfubaso}{rfubasoapio} \times 100\%$. Here, "rfu baso" indicated relative fluorescence units present in the basolateral sample and "rfu dose api" indicated

the relative fluorescence units present in the FD4 dose solution applied to the apical compartment at t=0. The acceptance criterion for this parameter is FD4 leakage ≤1% per hour for porcine ileum tissue under control conditions. The leakage of LDH into the apical and basolateral compartment was expressed as percentage of total LDH present in the (un-exposed) tissue segments using the following equation: $_{LDHleakage} = \frac{OD490api}{OD490totalLDH} \times 100\%$ and $leakage = \frac{OD490baso}{OD490botalLDH} \times 100\%$. Here, "OD490 api" or "OD490 baso" indicated the optical density at 490 nm measured in the apical or basolateral sample, respectively, and "OD490 total LDH" indicated the optical density at 490 nm measured in the tissue homogenate representing total LDH. The acceptance criterion for this parameter is LDH leakage \leq 3%/h of total LDH, during the length of the experiment under control conditions.

Statistical analysis was performed for the apparent permeability and the gene expression by ANOVA. All data was analysed using XLSTAT software package version 2014.5.03. All data was checked for normality. The individual well was the experimental unit. Data was analysed as a 2 x 3 factorial design for each condition. The model included the effects of test condition, presence of SEE challenge and time of sampling and the associated two- and three-way interactions. All data presented in the tables are expressed as least-square means with their standard errors of the mean. The probability level that denotes significance is P < 0.05; a numerical trend is P > 0.05 and P < 0.10. The Custom Design option of

Table 3 Porcine oligonucleotide primers used for quantitative real-time PCR

Gene	Accession no	Primer sequence (5' -> 3')	Product length (bp)	
GAPDH	NM_001206359.1	F: CAGCAATGCCTCCTGTACCA	72	
		R: ACGATGCCGAAGTTGTCATG		
CD17	XM_013996607.2	F: GCTATGTCAAGGTTAAAAAGCCTCT	113	
		R: GCTGGCATTGTACTGCACAC		
TNF-a	NM_214022.1	F: TCTGGCCCAAGGACTCAGAT	68	
		R: CTCGGCTTTGACATTGGCTAC		
DSG2	XM_003356392.4	F: TTGTGGCTGTCACCGAAGAATA	112	
		R: ATCATCTGCACTGGCTCGAC		
IL17a-R	XM_021092984.1	F: TGCCTGTGGTTCACATCGAG	104	
		R: CAGACGCTCGTTAGTGCTCA		
Caspase-1	NM_214162.1	AAATCTCACCGCTTCGGACAT	127	
		CTTCCCACAAATGCCAGCCT		
Reg-3γ	XM_021085605.1	TCTGCCTCTAGCACTGGGTT	100	
		TGCTGGGGAATCTTCACCTTTA		
IL-22	XM_001926156.1	ATGAGAGAGCGCTGCTACCTGG	112	
		GAAGGACGCCACCTCCTGCATGT		

the Design of Experiments function of JMP Statistical Software version 18.2.0 (JMP Statistical Discovery LLC) was used for further regression analysis. P_{app} was used as response variable with LG and ANE concentrations as fixed effects in a 3 x 3 factorial design with 3 replicates. The output of the experiment had a linear model fitted using least squares regression model.

Results

Tissue functionality markers

The ratio between the paracellular transport of [3H]-mannitol and transcellular [14C]-caffeine in the unchallenged, reference control was determined to verify tissue functionality. These were measured for all 3 timepoints from 60–120 mins, 120–240 mins and 240–300 mins. All unchallenged control samples had a $P_{\rm app}$ ratio between mannitol and caffeine of \geq 2 for all time points (data not shown), confirming the functionality of the tissue during the experiment. The SEE challenge resulted in significant increases of the $P_{\rm app}$ values for the paracellular transport of mannitol. These values increased ~7-fold for the control treatments, as was expected as SEE is known to damage the intestinal barrier integrity (see Fig. 1).

Tissue integrity and viability

The leakage of LDH from the tissue was used as a cell toxicity marker after 60, 120, 240 and 300 mins. The LDH leakage is associated with tissue viability, where low LDH leakage means that the tissue remains viable and structurally intact during the experiment and that there is no overt cell damage. The results of the LDH leakage are presented in Table 4 and Fig. 2. The LDH leakage was \leq 15%

Table 4 Source of variance for LDH, FD4 and P_{app}

	LDH	FD4	P_{app}
Condition (A)	ns	***	***
Treatment (B)	***	***	***
Time (C)		ns	***
AxB	*	***	***
AxC		**	***
ВхС		ns	***
$A \times B \times C$		ns	***

All parameters were incubated at two conditions and treated with 14 bioactives. FD4 and $P_{\rm app}$ were measured over 3 time points. LDH Lactate dehydrogenase leakage into the apical and basolateral compartment, FD4 FITC Dextran 4 permeability, $P_{\rm app}$ paracellular mannitol transport.

Ns non-significant

in 300 min (expressed cumulative) for the unchallenged as well as the SEE challenge condition, demonstrating the SEE did not affect cellular toxicity (P>0.10). An interaction was observed between condition x treatment (P<0.05). Differences in LDH were observed between the different test formulations (P<0.05), however, all results were in the acceptable range of LDH leakage of \leq 15% cumulative. For the three calcium controls, the individual LG and ANE, and LG 37.8/ANE 2.3 and

LG 37.8/ANE 4.5, the LDH leakage was higher in the unchallenged tissue compared to the challenged tissue, while for the other LG + ANE treatment groups, the LDH leakage was similar or lower in the unchallenged tissue compared to the challenged tissue.

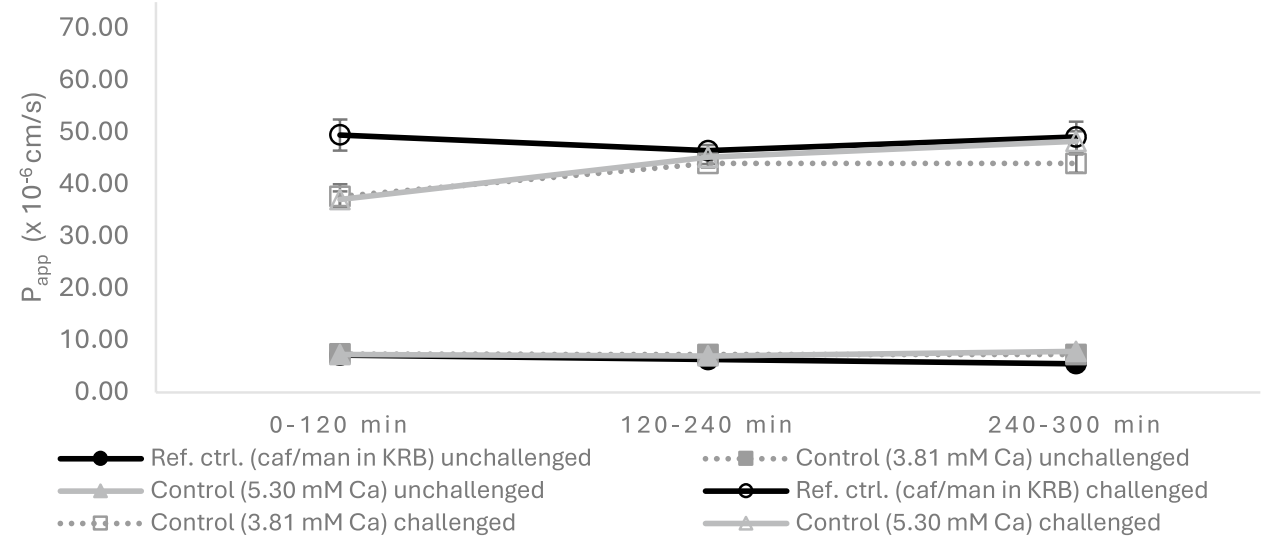


Fig. 1 Apparent permeability (Papp) of mannitol transport for time intervals 0–120, 120–240, and 240–300 min for 3 different control groups. Presented are the least square mean values with their standard errors, 4 replicates per treatment

^{*} significant at p < 0.05

^{**} significant at p < 0.01

^{***} significant at p < 0.001, respectively

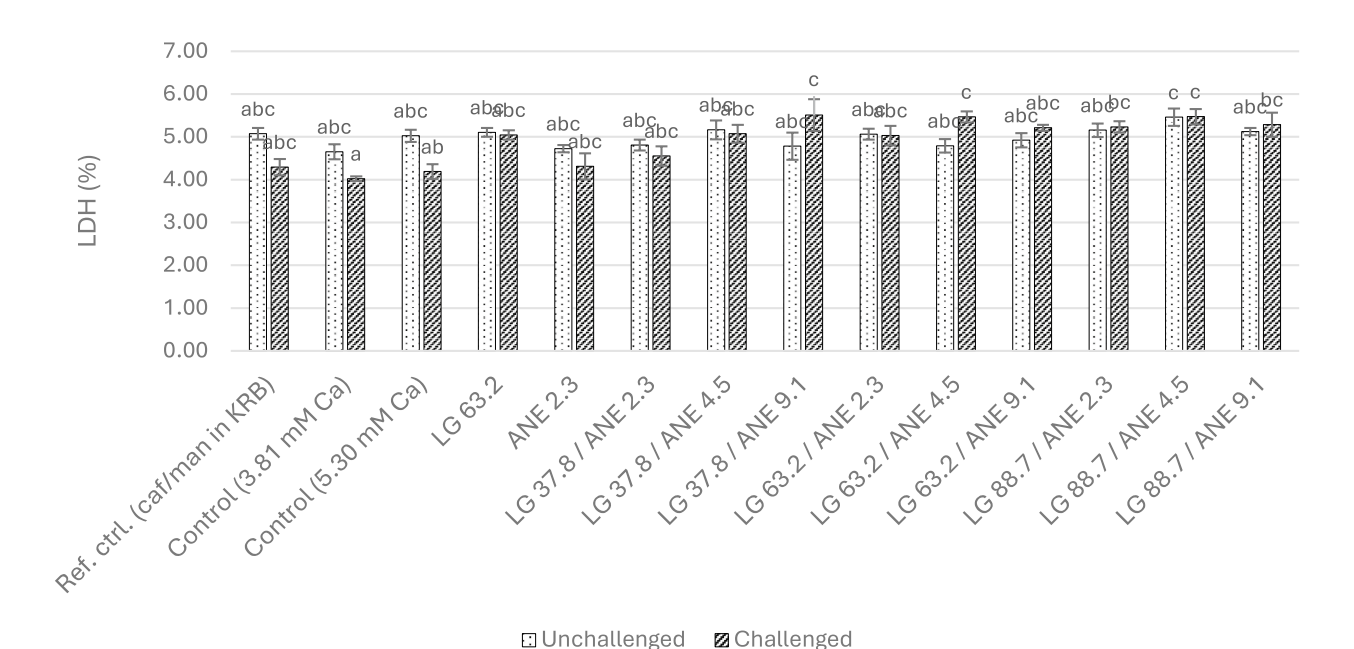


Fig. 2 LDH leakage (%) into apical and basolateral compartment after 300 min incubation as cumulative values. Unchallenged: not exposed to *Salmonella enterica enteriditis* challenge; Challenged: exposed to *Salmonella enterica enteriditis* challenge; LG: *Lithothamnion glaciale*; ANE: extract. Presented are the least square mean values with their standard errors, 4 replicates per treatment. Effects of treatment (*P*<0.001) and the interaction between condition x treatment (*P*<0.05) were observed

The permeability of FD4 was used as a barrier integrity marker for the intestinal tissue and was measured for all timepoints (t=60, t=120, t=240 and t=300 min). Transport of FD4 is measured to assess whether the intestinal epithelial barrier has sustained structural damage, as it only passes through the tissue when tight junctions are severely compromised. Summarized results are presented in Table 4 and Fig. 3. Supplementary Table 1 shows a detailed overview of the individual results with their differences for all timepoints and treatments. Fig. 3A presents the unchallenged and challenged calcium based controls, Fig. 3B presents the results for the single component LG 63.2 and ANE 2.3 in unchallenged and challenged conditions, and Fig. 3B shows the combined LG and ANE results for all 9 treatments in both unchallenged and challenged conditions. All unchallenged tissue had a FD4 permeability of $\leq 1\%$ /hour, meeting the assay criterion. Both the SEE challenge and the treatments affected SEE permeability (P<0.001). The SEE challenge condition affected FD4 permeability with a more than 3-fold higher FD4 permeability of 1.34±0.05%/hr, while the unchallenged tissue's FD4 permeability was 0.39±0.01 (P<0.001). An interaction between time and condition was observed (P<0.01) and between condition and treatment (*P*<0.001). The LG 37.8/ANE 2.3 and the LG 63.2/ANE 2.3 showed a much stronger response to the

challenge in their FD4 permeability compared to the other treatments.

Apparent permeability

The barrier function was measured by the transport of mannitol and represented as the P_{app}. The results are presented in Table 4 and Fig. 4. A significant effect of both condition, time and treatment was observed (*P*<0.0001; Table 4). Supplementary graph 1 shows the summarized P_{app} for all treatments at all time points, while Supplementary Table 2 shows all datapoints. The SEE challenge increased mannitol permeability \sim 7-fold, with P_{app} being 6.77±0.08 in the unchallenged samples and 45.60±0.37 in the challenged samples (P<0.0001). Interactions for condition x time (P<0.001), condition x treatment (P<0.0001), time x treatment (P<0.0001), and condition x time x treatment (P<0.0001) were observed. Based on this analysis and the increase in FD4 after 240 mins, further analysis was performed at this time point. Figure 4 presents the effect of SEE challenge and the treatments at this timepoint. Figure 4 shows that the LG 37.8/ANE 2.3 and the LG 63.2/ANE 2.3 treatment group show a reduced P_{app} compared to the other treatment groups following the SEE challenge. The interaction between condition x time x treatment indicated that the combination of LG and ANE at the low ANE dose (the LG 37.8/ANE 2.3 and the LG 63.2/ANE 2.3 treatment group) had a strong

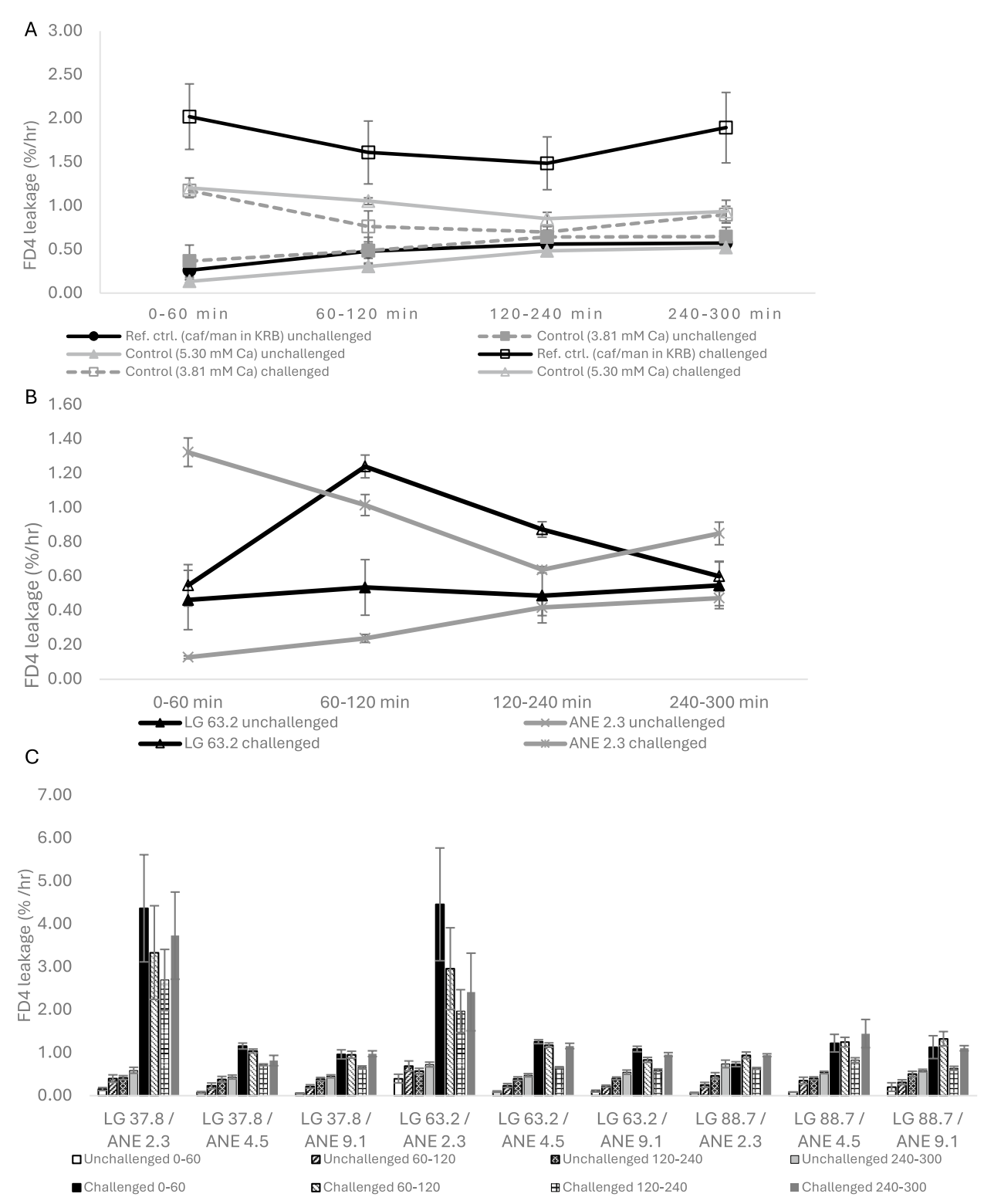


Fig. 3 FD4 permeability for time intervals 0–60, 60–120, 120–240, and 240–300 minutes. **A** control treatment groups; **B** single components LG and ANE; **C** combined components LG + ANE without and with *Salmonella enterica enteriditis* challenge. LG: *Lithothamnion glaciale*; ANE: *Ascophyllum Nodosum* extract. Presented are the least square mean values with their standard errors, 4 replicates per treatment

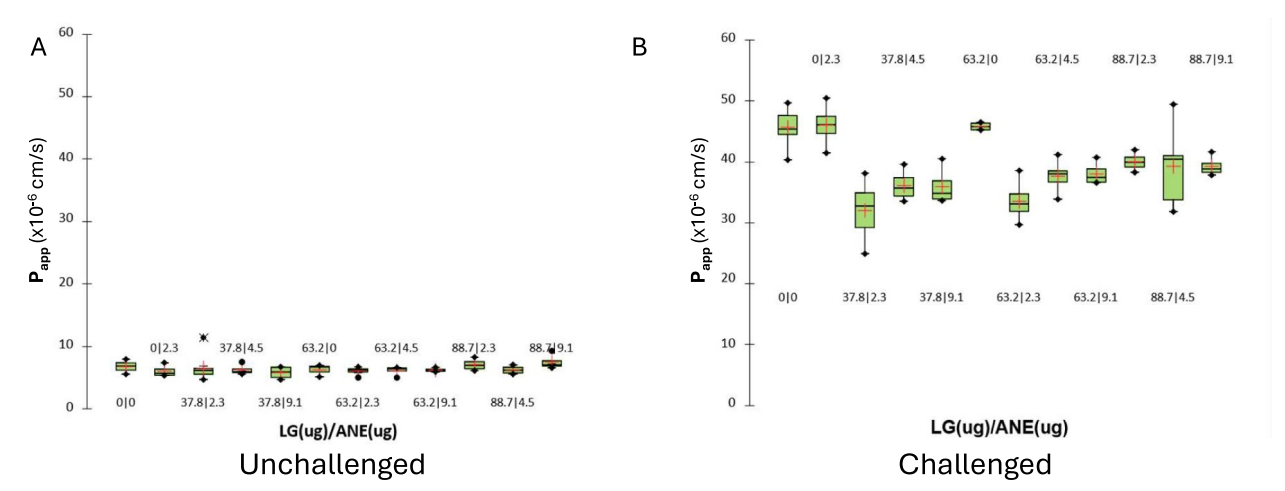


Fig. 4 Apparent permeability P_{app} of mannitol transport for the combined LG and ANE treatments without and with SEE challenge at 240 minutes. **A** Treatment groups in unchallenged conditions; **B** Treatment groups in challenged conditions. LG: Lithothamnion glaciale, ANE Ascophyllum Nodosum extract, SEE Salmonella enterica enteriditis. Presented are the least square mean values with their standard errors, 4 replicates per treatment

effect on reducing the negative effects of the SEE challenge (P<0.001), while this was not seen at the individual LG or ANE inclusion or the control levels. A further linear regression analysis was performed, as shown in Fig. 5 (P<0.01). This Contour plot shows how the different doses of LG and ANE interact with each other and which combinations of components results in the lowest apparent permeability figures. This graph indicates that the 2.3 μ g inclusion of ANE results in the strongest reduction of the apparent permeability, together with the 37.8 μ g inclusion of LG.

Histology

The images of the formalin fixed and wax embedded ileal tissue after microtomy and staining for histological examination are presented in Fig. 6. Images of the control tissue before (Fig. 6B) and after the SEE challenge (Fig. 6D), as well as the LG 63.2/ANE 2.3 tissue before (Fig. 6C) and after the challenge (Fig. 6E) are presented. There was no effect of treatments on the cytotoxicity of the tissue. The SEE challenge had a negative effect on the structure of the tissue. The control image at 0 hours (Fig. 6A) shows a clear structure, with intact villi and crypts. After 5 hours, clear changes can be observed in the tissue (Fig. 6D and E). In the unchallenged tissue, the tops of the villi appear to be slouched off and the cells are poorly defined. This can be attributed to the time in the InTESTineTM model and indicates tissue necrosis. The challenged tissue after 5 hr incubation shows severe damage, both in the control and LG 63.2/ANE 2.3 treatment. This is evidenced by the broken villi structure and crypt atrophy. The increased purple nuclear staining between the different time points highlights an infiltration of the immune cells into the tissue, indicating an inflammatory response to the SEE challenge. Collectively, these findings underline a profound impact of the SEE challenge on tissue morphology.

Gene expression profiles

The gene expression profiles of CDH17, TNF-α, DSG-2, IL17a-R, IL-22, Caspase-1 and Reg3-γ are presented in Table 5. Following the P_{app} challenge, the two best performing treatments were submitted to the gene expression analysis. These treatments were LG 37.8/ANE 2.3 and LG 63.2/ANE 2.3. In the control samples, the SEE challenged conditions resulted in a reduced expression of TNF- α (P<0.01) and caspase-1 (P<0.01). In the unchallenged samples, the expression of CDH17, DSG-2, TNFα, IL-22, Caspase-1 and Reg3-y were affected by the test treatments (P<0.05). The inclusion of LG 63.2, ANE 2.3 and LG 63.2/ANE 2.3 increased the expression of CDH17, while LG + ANE1 was not different from either control or ANE alone (P<0.001). For DSG-2, the inclusion of ANE 2.3 alone reduced the expression of this gene compared to the control, LG 63.2, and LG 63.2/ANE 2.3 (P<0.001). The TNF-α expression was reduced in the LG 63.2 and LG 63.2/ANE 2.3 treatments compared to all others (P<0.001). Caspase-1 expression was increased in the LG 63.2/ANE 2.3 treatment compared to the Control, LG 63.2, and LG 37.8/ANE 2.3 treatment (*P*<0.001). The inclusion of LG 37.8/ANE 2.3 and LG 63.2/ANE 2.3 increased IL-22 expression compared to the Control and LG 63.2 treatment, with the ANE 2.3 treatment being reduced compared to the LG 37.8/ANE 2.3 (P<0.001). ANE 2.3 and LG 63.2/ANE 2.3 inclusion increased Reg3-y expression compared to the Control treatment (P < 0.01).

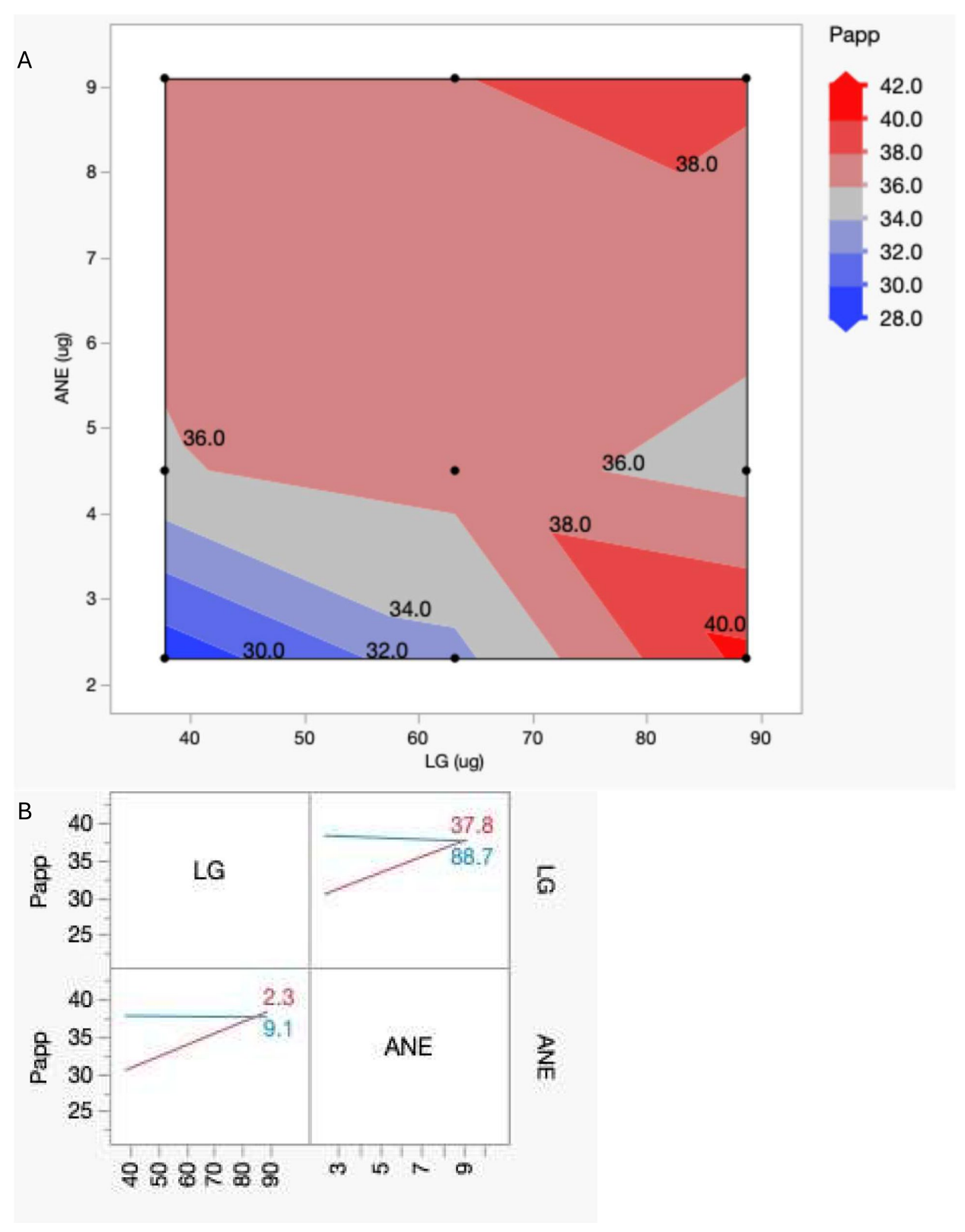


Fig. 5 Regression analysis for LG and ANE treatment groups apparent permeability (P_{app}) without and with SEE challenge. **A** Contour plot; **B** Interaction profiles. Predicted RMSE for the linear regression: 3.1626; $R^2 = 0.45$; P-value < 0.01. LG: Lithothamnion glaciale; ANE: Ascophyllum Nodosum extract; SEE: Salmonella enterica enteriditis

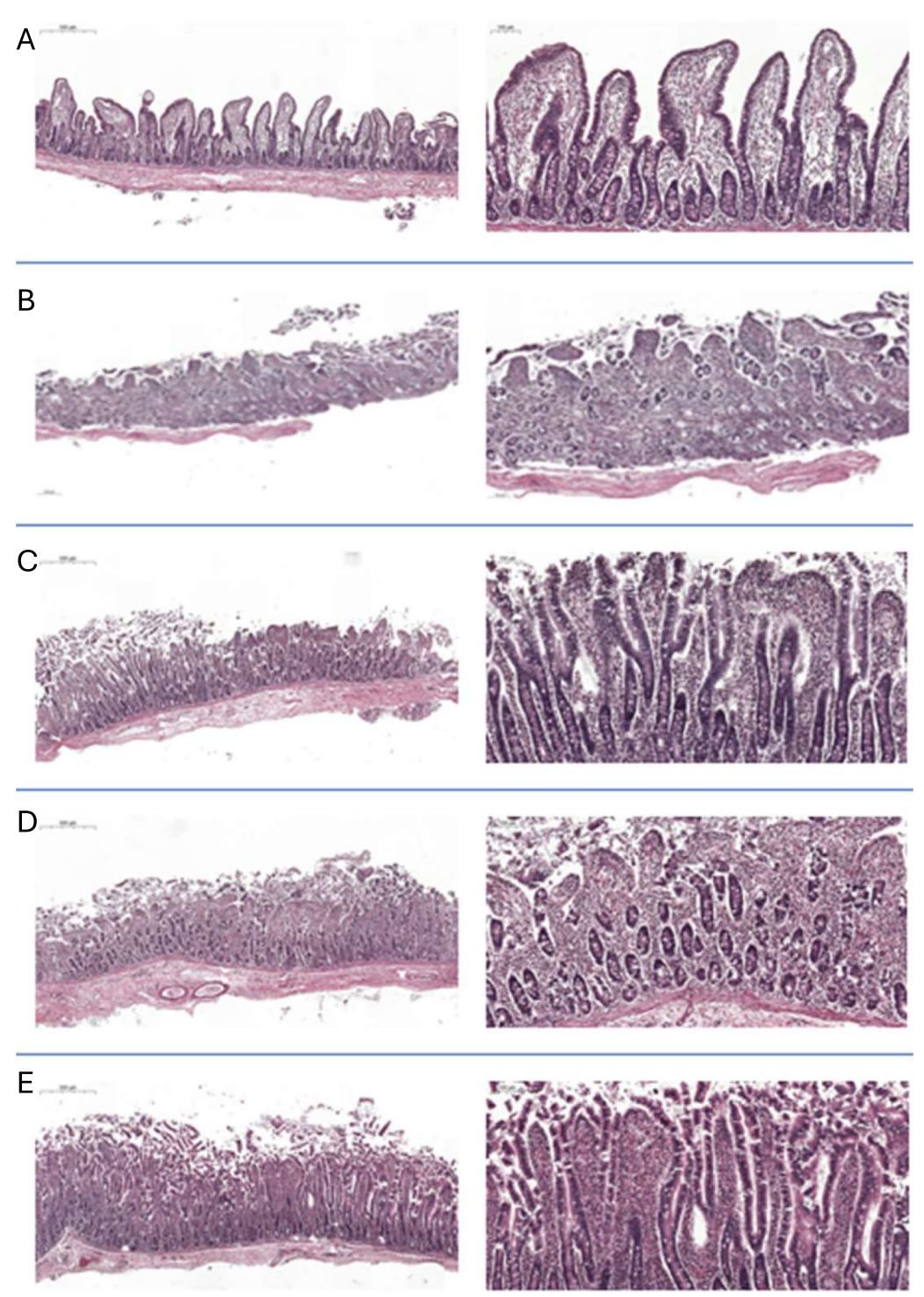


Fig. 6 Histological analysis of tissue following inTESTineTM incubation. **A** Blanc at 0 hr; **B** Control at 5 hrs; **C** LG 63.2/ANE 2.3 treatment at 5 hrs; **D** Control + SEE challenge at 5 hrs; **E** LG 63.2/ANE 2.3 + SEE challenge at 5 hrs. SEE: Salmonella enterica enteriditis; LG: Lithothamnion glaciale; ANE: Ascophyllum Nodosum extract

Table 5 Relative expression of a panel of genes for unchallenged and challenged control and test conditions

	CDH17	DSG-2	TNF-α	IL17 A-R	Caspase 1	II-22	Reg3-γ
Control 3.8 mM Ca							
Unchallenged	1.10	1.11	1.01	1.02	0.95	0.93	0.88
Challenged	0.95	1.15	0.82	1.24	0.59	0.88	0.83
SEM	0.128	0.169	0.410	0.120	0.080	0.097	0.042
P-value	ns	ns	**	ns	**	ns	ns
Unchallenged							
Control (3.8 mM Ca)	1.10a	1.11bc	1.01b	1.02	0.95a	0.93a	0.92a
LG 63.2	9.51c	1.50c	0.29a	1.23	1.33a	0.81a	1.44ab
ANE 2.3	4.46b	0.52a	1.12b	1.17	1.55ab	1.36ab	1.70b
LG 37.8/ ANE 2.3	1.83ab	0.84ab	0.98b	1.26 a	0.94a	2.06c	1.52ab
LG 63.2/ ANE 2.3	10.17c	1.25bc	0.43a	1.02	2.25b	1.75bc	2.05b
SEM	0.674	0.144	0.048	0.087	0.183	0.162	0.189
P-value	***	***	***	ns	***	***	**
Challenged							
Control (3.8 mM Ca)	0.95a	1.15	0.82b	1.54	0.59a	0.88a	0.83a
LG 63.2	5.15c	0.63	0.34a	1.03	0.96ab	1.13ab	0.96b
ANE 2.3	5.91c	0.76	0.40a	1.52	1.25b	1.03a	0.90b
LG 37.8/ ANE 2.3	3.17ab	0.67	0.85b	0.97	0.77a	1.61c	0.68a
LG 63.2/ ANE 2.3	3.95bc	0.72	0.40a	1.43	1.22b	1.49bc	1.64c
SEM	0.782	0.149	0.028	0.190	0.106	0.115	0.094
<i>P</i> -value	***	ns	***	ns	**	**	***

(Least square mean values with their standard errors, 4 replicates per treatment)

CDH17 Cadherin 17, DSG2 Desmoglein 2, TNF-α tumour necrosis factor alpha, IL-17a-R interleukin 17 receptor A, IL-22 Interleukin 22, Reg3-γ regenerating islet-derived protein-3 γ, LG Lithothamnion glaciale, ANE Ascophyllum Nodosum extract

Ns non-significant

a,b,c Mean values with unlike superscript letters were significantly different (P<0.05)

In the SEE challenged conditions, CDH17, TNF- α , IL-22, caspase 1 and Reg3-y expression was affected by the test treatments. Both LG 63.2 and ANE 2.3 individually increased the expression of CDH-17 compared to the control treatment and LG 37.8/ANE 2.3, with LG 63.2/ANE 2.3 being intermediate (P<0.001). The TNF- α expression was reduced when LG 63.2, ANE 2.3 or LG 63.2/ANE 2.3 was included compared to the control and LG 37.8/ANE 2.3 treatment (*P*<0.001). For Caspase-1, the inclusion of ANE 2.3 and LG 63.2/ANE 2.3 increased its expression compared to the control and LG 37.8/ANE 2.3 treatment (P<0.01). Interleukin-22 expression was increased when LG 37.8/ANE 2.3 or LG 63.2/ANE 2.3 were added in comparison to the control and ANE 2.3 treatment. The LG 63.2/ANE 2.3 treatment increased Reg3-y expression compared to all other treatments, while LG 63.2 and ANE 2.3 alone increased the expression in comparison to the control and LG 37.8/ANE 2.3 treatment (*P*<0.001).

Discussion

An intact, strong gut barrier is of vital importance for healthy functioning of the intestinal tract and subsequent animal health and performance. If the gut barrier is impaired, this may result in toxins, bacteria and viruses, and foodborne immunostimulants entering the bloodstream resulting in tissue damage and an inflammatory response. It has been reported that LG and ANE individually have a positive influence on the gut barrier [9, 14]. Therefore, the current research investigated the effect of LG and ANE and their combination on gut barrier functioning and markers of inflammation in a previously reported ex vivo model [16, 17, 23]. The ex vivo model was chosen to allow for using a fully functional organ structure, which is not available in an in vitro cell culture model. With the current methodology, all tested conditions and substances were tested using tissue from a single pig, reducing the number of animals required and reducing the between animal variability.

^{*} significant at p < 0.05

^{**} significant at p < 0.01

^{***} significant at p < 0.001, respectively

The different test components had variable effect on apparent permeability (Papp) under the different conditions. The experimental setup and tissue was suitable for use as measured by the P_{app} ratio for the control treatments being greater than 2, showing that there was sufficient tissue viability and functionality. The expected effect of the SEE challenge was seen in the experiment, showing a disrupted barrier with an average increase of the P_{app} value of approximately 7 fold for the paracellular transported mannitol when the SEE challenge was applied to the tissue. This demonstrates the increased paracellular transport as a result of disruptions in the tight junction structures and thus a more permeable gut barrier. It has been described extensively in literature that the gene expression of tight junctions is reduced during infestation of epithelial cells by Salmonellae [24, 25]. Hence, this leads to an increase in gut permeability, as is observed in the current study. These results suggest that the methodology effectively induces an impaired gut barrier, therefore confirming its suitability for the current research questions.

The obtained gut permeability results demonstrate that there was a significant difference in the response to the different treatments in the different time points. This was especially clear in the incubations that were exposed to the SEE challenge. The measuring point at 120 mins showed that there is a certain incubation time required before the cells respond to the different treatments, explaining the more limited effects of the different treatments on the P_{app} at the 120 min time point. The modulation of the immune cells and production of tight junction proteins has been achieved at the 240 mins timepoint, showing the most effective responses and reduced P_{app} for certain treatments. At the 300 mins time point, the tissue appears to be reaching its lifespan and there is a reduced response again for all test substances. This leads to an increase in P_{app} at the 300 min time point. SEE is known to have a strong effect on the gut barrier [24] and cause subsequent inflammation. Hence, it appears that the gut barrier rupture and inflammatory responses caused by the SEE challenge affected the tissue strongly and subsequently caused damage to the tissue, reducing its lifespan in the InTESTineTM system. Nevertheless, the different treatments did not affect the cell viability and no signs of cytotoxicity were observed. For future research, it may be beneficial to reduce the total experimental time to 4 hrs maximum in case of the SEE challenge.

Different beneficial effects of the test substances on gut permeability as measured by P_{app} of mannitol were observed in the SEE challenged conditions, whereas the treatments did not affect mannitol permeability in the unchallenged control conditions. The individual LG or

ANE treatment did not affect the gut permeability values, but certain combinations of LG and ANE had a positive effect on reducing the gut permeability. The results indicate that there is an optimum dose of both LG and ANE in order to maximise this positive effect. Following the regression analysis, low level inclusion of the combination of LG and ANE (37.8 and 63.2 µg LG combined with 2.3 µg of ANE) had a significantly reduced permeability compared to the 3 calcium level controls, highlighting that the effects were additional to any benefits of calcium alone. Considering the results from the gene expression analysis, it is hypothesized that the combination of LG and ANE may lead to a reduced colonization of the epithelial cells by SEE, subsequently attenuating the inflammatory response and reducing the disruption of tight junctions. This will maintain the gut barrier and thus reduce permeability.

There is no research available looking at the combination of LG and ANE on gut barrier permeability to the best of the authors' knowledge. However, there is evidence of the potential of both LG and ANE individually to enhance the gut barrier. Zou et al. [26] showed that extracts similar in composition to the ANE of the current study had a positive effect on the gut barrier of newly weaned piglets. The authors reported increased levels of the tight junction proteins, zonula occludens protein-1 and Claudin-1 in the jejunum and Occludin in jejunum as well as in the duodenum and ileum. Also, the paracellular transport of D-lactate was significantly reduced. These are all indicators for an enhanced intestinal barrier function. Similar results were observed by Hwang et al. [14], who reported an improved gut barrier function in an in vitro experiment using a fucoidan-rich extract in Caco-2 cells challenged with LPS. Studies with LG have consistently shown upregulation of tight junction and adhesion proteins, particularly desmosomal proteins, in both diseased and in vitro models [8-10]. The inclusion of LG into either test subjects with barrier affecting diseases or into in vitro models reveals a distinct mechanism, where particularly desmosomes are affected. These proteins are crucial for preserving the structural integrity of intestinal epithelial cells. LG appears to promote epithelial integrity at a deeper structural level, as reflected by increased desmosome numbers and basement membrane-associated protein expression, including laminins and cadherins [9, 10]. The aforementioned observations suggest that ANE primarily affects the apical tight junction complex, while LG influences cell-matrix and desmosomal structures closer to the basal region. Although these spatial distinctions in mode of action are biologically plausible and supported by proteomic and ultrastructural evidence from prior studies, the current dataset

does not directly measure apical versus basal compartment-specific effects. Thus, while synergy between LG and ANE in enhancing barrier function was observed, further targeted investigation is needed to definitively localize their site of action.

Tissue gene expression was analysed to evaluate the effect on expression of genes associated with the immune response following an SEE challenge and genes associated with gut barrier structural components. The selected genes were based on prior studies involving ANE and/or LG. Notably, Aslam et al. [10] showed that LG upregulated several gut barrier proteins in ulcerative colitis patients, particularly those involved in cellcell adhesion such as tight junctions, adherens junctions, and desmosomes. These findings prompted investigation of Cadherin-17 and Desmoglein-2 in the current study. Cadherin-17 expression was upregulated upon inclusion of the test substances in both challenged and unchallenged conditions. Both individual treatment with LG or ANE, as well as their combination LG 63.2/ANE 2.3, improved Cadherin-17 expression. In healthy tissue, increased Cadherin-17 expression is correlated with a stronger gut barrier, facilitating stronger adhesion to the basal membrane [27].

In the unchallenged tissue, during the incubation with LG and LG 63.2/ANE 2.3, the Cadherin-17 expression got upregulated while TNF-α got downregulated, showing a reduced inflammatory response and disruption of the tight junctions and better connection to the basal membrane. The reduction in TNF- α expression observed in this study aligns with earlier research showing anti-inflammatory effects of LG in both healthy and challenged tissues [10, 28]. Since TNF- α plays an early role in the inflammatory cascade and stimulates IL-6 production, which is often linked to activation of the $NF-\kappa\beta$ pathway, these findings point toward a dampening of upstream inflammatory signals. Although the NF-κβ pathway itself wasn't measured in this study, the pattern of cytokine responses suggests that LG may influence this pathway, as reported in previous work [10, 28].

Although SEE is a well-characterized inducer of intestinal inflammation, the current study did not observe upregulation of the selected inflammatory markers in the challenged control group. In fact, TNF- α and Caspase-1 expression was reduced following SEE exposure, and no changes were observed in the other measured genes compared to the unchallenged control. This absence of a clear pro-inflammatory response contrasts with common expectations for acute mucosal infection models. Recent studies suggest that the early stages of *Salmonella* infection may involve active suppression or temporal delay of

inflammatory signalling to facilitate epithelial invasion and intracellular survival. For instance, Kawasaki et al. [29] demonstrated in a bovine ileal organoid model that although SEE caused epithelial disruption and intracellular bacterial invasion, TNF-α expression was either modest or delayed, and downstream cytokine secretion remained low in the early infection phase. This aligns with findings by Worley [30], who reviewed that several Salmonella Type III secretion system (T3SS) effectors actively inhibit NF-κβ activation and TNF-α signalling to overthrow host immune detection during early colonization. The absence of an inflammatory response in the challenged control group of the current study may reflect a biologically relevant strategy employed by SEE to evade host immune activation during the initial infection phase, since tissue for the gene expression analysis was recovered 5 hours post-infection. The immunomodulatory effects observed with LG, ANE and LG + ANE supplementation most likely represents a primed or restored immune response that counteracts this early immune suppression by SEE.

Incubation with SEE will activate the immune response through various mechanisms, such as the recognition of lipopolysaccharides or flagella present on the bacterial outer membrane [31, 32]. All Salmonella enterica serovars express flagella, which are detected through at least two pathways: 1) extracellular flagella are recognized as microbial associated molecular patterns (MAMPs) by Toll-like receptor 5, which triggers the previously discussed NF-κβ signalling pathway; and 2) cytosolic flagella are recognized by the NaiP5-NaiP6/NlrC4/Caspase-1 pathway, which contains an inflammasome that activates IL-1β and IL-18 [33-35]. Upon activation of IL-18 production, IL-22 is subsequently activated. Interleukin 22, a part of the IL-10 family of cytokines, plays a critical role in defending the host at mucosal surfaces and tissue repair during pathogenic infections [36, 37]. Interleukin 22 induces the production of multiple antimicrobial proteins such as Reg3-y, which is a C-type lectin and binds to peptidoglycans on the bacterial membrane, enhancing the antimicrobial defence at epithelial surfaces. These antimicrobial proteins are not only regulated by IL-22 but also through NF-κβ pathway activation. As such, they may serve as biomarkers of inflammation since they are produced in response to the major inflammatory signalling pathways [36].

In the present study, the test substances elicited different immune responses. In SEE challenged tissue, the inclusion of LG 63.2/ANE 2.3 showed an increase in the relative expression of both Caspase-1, IL-22, and Reg3-γ, while ANE alone upregulated Caspase-1 and Reg3-γ.

These findings suggest a potentially more efficient inflammatory response to the SEE challenge, which may result in faster recovery in vivo. This is consistent with prior studies indicating an interaction between the NaiP5-NaiP6/NlrC4/Caspase-1 pathway and ANE supplementation in pigs. However, these studies reported a reduced activation of this pathway and its associated products following an experimental infection of *Salmonella Typhimurium* and a subsequent recovery period [15, 38, 39]. In these studies, pigs demonstrated more rapid recovery, better growth, and improved feed efficiency when supplemented with ANE. Bouwhuis et al. [15] proposed that bioactive compounds in ANE could enhance the immune response to a S. Typhimurium challenge, leading to a better recovery and health outcomes.

The inclusion of ANE, both on its own as well as LG 63.2/ANE 2.3, also affected TNF- α expression. Both bioactives in the ANE, laminarin and fucoidan, have been associated with anti-inflammatory effects in pigs before, both during the weaning challenge as well as a *Salmonella* infection [15, 40, 41]. These bioactives interact with pattern recognition receptors such as Toll-like receptor 4 and 6 and subsequently reduce the activation of the NF κ B pathway and Myd88 response [26].

Consequently, the results of this study indicate that both LG and ANE modulate the inflammatory response in intestinal epithelial cells during the SEE challenge albeit through different mechanisms. The presence of LG and ANE seem to have primed the immune cells to react in a more rapid or stronger response. Both LG and ANE appear to influence the activation of the NF-κβ pathway, resulting in a reduction in immune system activation, Additionally, ANE also modulates the NaiP5-NaiP6/ NlrC4/Caspase-1 inflammasome pathway and its associated molecules. The observed synergistic effects between LG and ANE, particularly in their immunomodulatory role, warrant further investigation to understand the underlying mechanisms. Immune priming, leading to a more efficient recovery, seems plausible but will require further research. Furthermore, the results for both the mannitol transport and the gene expression indicate that LG 63.2/ANE 2.3 yields the most robust effects.

Conclusion

The efficacy of two different marine sources of bioactives, LG and ANE, and their combinations were evaluated in an ex vivo experiment. The experiment entailed an SEE challenge which was successful in causing barrier damage with increased permeability measured. The inclusion of a combination of LG + ANE resulted in reduced gut permeability following the SEE challenge, with the optimum ratio being LG 37.8/ ANE 2.3 and LG 63.2/ANE 2.3. The gene expression analysis demonstrated that LG improved

the expression of Cadherin-17 in both challenged and unchallenged tissue and displayed anti-inflammatory activity with a reduction in TNF- α expression. ANE inclusion resulted in improved Cadherin-17 and reduced TNF- α expression, while increasing the expression of Caspase-1 and Reg3- γ . The combination of LG at 63.2 μg and ANE at 2.3 μg had a synergistic benefit on the barrier integrity and showed a faster response on the SEE challenge by activation of Caspase-1, IL-22 and Reg3- γ . This indicates a potential for a faster recovery from infection exposure in vivo.

Supplementary Information

The online version contains supplementary material available at https://doi.org/10.1186/s12917-025-04832-7.

Supplementary Material 1.

Supplementary Material 2.

Supplementary Material 3.

Acknowledgements

Not applicable.

Authors' contributions

MAB: conceptualization, data curation, data analysis, writing of original draft. IHGN, EvdS: conceptualization, supervision of data curation and preparation of data analysis, reviewed manuscript. SOC: conceptualization, data analysis, reviewed manuscript. All authors have read and approved the final manuscript.

Funding

This research was funded by Marigot Ltd t/a Celtic Sea Minerals.

Data availability

The datasets used and/or analysed during the current study are available from the corresponding author on reasonable request.

Declarations

Ethics approval and consent to participate

This research was conducted following the European Directive 2010/63/EU and the regulations in force in the Netherlands for the care and use of animals in research. The experimental procedures were evaluated and approved by the Ethical Committee on Animal Experiments (Ethische Toetsing Dierproeven of TNO).

Consent for publications

Not applicable.

Competing interests

MAB and SOC are employed by Celtic Sea Minerals.

Author details

¹Celtic Sea Minerals, Marigot Research Centre, Clash Road, Tralee, Co. Kerry, Ireland. ²The Netherlands Organization for Applied Scientific Research (TNO), Sylviusweg 71, Leiden 2333 BE, the Netherlands. ³Centre for Applied Bioscience Research, Munster Technology University, Clash Road, Tralee, Co. Kerry, Ireland.

Received: 20 December 2024 Accepted: 15 May 2025 Published online: 29 May 2025

References

- Wijtten PJA, Van Der Meulen J, Verstegen MWA. Intestinal barrier function and absorption in pigs after weaning: a review. Br J Nutr. 2011:105(7):967–81.
- Lallès JP, Montoya CA. Dietary alternatives to in-feed antibiotics, gut barrier function and inflammation in piglets post-weaning: where are we now? Anim Feed Sci Technol. 2021;274:114836. Elsevier B.V.
- Moeser AJ, Pohl CS, Rajput M. Weaning stress and gastrointestinal barrier development: implications for lifelong gut health in pigs. Anim Nutr. 2017;3:313–21. KeAi Communications Co.
- Pluske JR, Turpin DL, Kim JC. Gastrointestinal tract (gut) health in the young pig. Anim Nutr. 2018;4:187–96. KeAi Communications Co.
- Robbins LA, Green-Miller AR, Lay DC, Schinckel AP, Johnson JS, Gaskill BN. Evaluation of sow thermal preference across three stages of reproduction. J Anim Sci. 2021;99(8):skab202.
- Vermeer HM, Aarnink AJA. Review on heat stress in pigs on farm. Wageningen, the Netherlands; 2023. https://doi.org/10.5281/zenodo.7620726.
- Mayorga EJ, Ross JW, Keating AF, Rhoads RP, Baumgard LH. Biology of heat stress; the nexus between intestinal hyperpermeability and swine reproduction. Theriogenology. 2020;154:73–83. Elsevier Inc.
- Varani J, McClintock SD, Aslam MN. Cell-matrix interactions contribute to barrier function in human colon organoids. Front Med (Lausanne). 2022:10:9
- Aslam MN, McClintock SD, Jawad-Makki MAH, Knuver K, Ahmad HM, Basrur V, et al. A multi-mineral intervention to modulate colonic mucosal protein profile: results from a 90-day trial in human subjects. Nutrients. 2021;13(3):1–21.
- Aslam MN, McClintock SD, Attili D, Pandya S, Rehman H, Nadeem DM, et al. Ulcerative colitis-derived colonoid culture: a multi-mineral-approach to improve barrier protein expression. Front Cell Dev Biol. 2020;23:8.
- You L, Gong Y, Li L, Hu X, Brennan C, Kulikouskaya V. Beneficial effects of three brown seaweed polysaccharides on gut microbiota and their structural characteristics: an overview. Int J Food Sci Technol. 2020;55:1199– 206. Blackwell Publishing Ltd.
- 12. Wang HMD, Li XC, Lee DJ, Chang JS. Potential biomedical applications of marine algae. Bioresour Technol. 2017;244:1407–15. Elsevier Ltd.
- Okolie CL, Subin SR, Udenigwe CC, Aryee ANA, Mason B. Prospects of brown seaweed polysaccharides (BSP) as prebiotics and potential immunomodulators. J Food Biochem. 2017;41:1-12
- Hwang PA, Phan NN, Lu WJ, Hieu BTN, Lin YC. Low-molecular-weight fucoidan and high-stability fucoxanthin from brown seaweed exert prebiotics and anti-inflammatory activities in Caco-2 cells. Food Nutr Res. 2016;2:60.
- Bouwhuis MA, McDonnell MJ, Sweeney T, Mukhopadhya A, O'Shea CJ, O'Doherty JV. Seaweed extracts and galacto-oligosaccharides improve intestinal health in pigs following Salmonella Typhimurium challenge. Animal. 2017;11(9):1488–96.
- Westerhout J, Van De Steeg E, Grossouw D, Zeijdner EE, Krul CAM, Verwei M, et al. A new approach to predict human intestinal absorption using porcine intestinal tissue and biorelevant matrices. Eur J Pharm Sci. 2014;15(63):167–77.
- Stevens LJ, van Lipzig MMH, Erpelinck SLA, Pronk A, van Gorp J, Wortelboer HM, et al. A higher throughput and physiologically relevant two-compartmental human ex vivo intestinal tissue system for studying gastrointestinal processes. Eur J Pharm Sci. 2019;1:137.
- Quille P, Higgins T, Neville EW, Regan K, O'Connell S. Evaluation and development of analytical procedures to assess buffering capacity of carbonate ruminant feed buffers. Animals. 2024;14(16):2333.
- Goñi O, Quille P, O'Connell S. Ascophyllum nodosum extract biostimulants and their role in enhancing tolerance to drought stress in tomato plants. Plant Physiol Biochem. 2018;1(126):63–73.
- O'driscoll K, O'gorman DM, Taylor S, Boyle LA. The influence of a magnesium-rich marine extract on behaviour, salivary cortisol levels and skin lesions in growing pigs. Animal. 2013;7(6):1017–27.
- 21. Bouwhuis M, Frio A, O'Connell S. P199. The effect of a marine mineral complex on growth performance of weaned piglets. Anim Sci Proc. 2022;13(2):219–20.
- 22. Walsh AM, Sweeney T, O'Shea CJ, Doyle DN, O'Doherty JV. Effect of supplementing varying inclusion levels of laminarin and fucoidan on growth performance, digestibility of diet components, selected faecal microbial populations and volatile fatty acid concentrations in weaned pigs. Anim

- Feed Sci Technol. 2013;183(3–4):151–9. https://doi.org/10.1016/j.anifeedsci.2013.04.013.
- 23. Westerhout J, Bellmann S, van Ee R, Havenaar R, Leeman W, van de Steeg E, et al. Prediction of oral absorption of nanoparticles from biorelevant matrices using a combination of physiologically relevant in vitro and ex vivo models. J Food Chem Nanotechnol. 2017;03(04):111–9.
- Guttman JA, Finlay BB. Tight junctions as targets of infectious agents. Biochim Biophys Acta Biomembranes. 2009;1788:832–41.
- 25. Paradis T, Bègue H, Basmaciyan L, Dalle F, Bon F. Tight junctions as a key for pathogens invasion in intestinal epithelial cells. Int J Mol Sci. 2021;22:1–21. MDPI AG.
- Zou T, Yang J, Guo X, He Q, Wang Z, You J. Dietary seaweed-derived polysaccharides improve growth performance of weaned pigs through maintaining intestinal barrier function and modulating gut microbial populations. J Anim Sci Biotechnol. 2021;12(1):28.
- Lechuga S, Ivanov AI. Disruption of the epithelial barrier during intestinal inflammation: quest for new molecules and mechanisms. Biochim Biophys Acta Mol Cell Res. 2017;1864:1183–94. Elsevier B.V.
- 28. O'Gorman DM, Naderi Z, Yeganeh A, Malboosbaf R, Eriksen EF.

 Disease-modifying adjunctive therapy of osteopenia and osteoporosis with a multimineral marine extract, LithoLexal[®] Bone. Osteology. 2023:3(1):22–32.
- Kawasaki M, McConnel CS, Burbick CR, Ambrosini YM. Pathogen-epithelium interactions and inflammatory responses in Salmonella Dublin infections using ileal monolayer models derived from adult bovine organoids. Sci Rep. 2024;14(1):11479.
- Worley MJ. Salmonella type III secretion system effectors. Int J Mol Sci. 2025;26:2611.
- 31. Mukherjee S, Hooper LV. Antimicrobial defense of the intestine. Immunity. 2015;42:28–39.
- Krzyżewska-Dudek E, Kotimaa J, Kapczyńska K, Rybka J, Meri S. Lipopolysaccharides and outer membrane proteins as main structures involved in complement evasion strategies of non-typhoidal Salmonella strains. Mol Immunol. 2022;1(150):67–77.
- 33. Vijay-Kumar M, Wu H, Jones R, Grant G, Babbin B, King TP, et al. Flagellin suppresses epithelial apoptosis and limits disease during enteric infection. Am J Pathol. 2006;169(5):1686–700.
- 34. Lai MA, Quarles EK, López-Yglesias AH, Zhao X, Hajjar AM, Smith KD. Innate immune detection of flagellin positively and negatively regulates salmonella infection. PLoS One. 2013;8(8):e72047.
- Ménard S, Lacroix-Lamandé S, Ehrhardt K, Yan J, Grassl GA, Wiedemann A. Cross-talk between the intestinal epithelium and Salmonella typhimurium. Front Microbiol. 2022;13:906238. Frontiers Media S.A.
- 36. Behnsen J, Jellbauer S, Wong CP, Edwards RA, George MD, Ouyang W, et al. The cytokine IL-22 promotes pathogen colonization by suppressing related commensal bacteria. Immunity. 2014;40(2):262–73.
- Zheng Y, Valdez PA, Danilenko DM, Hu Y, Sa SM, Gong Q, et al. Interleukin-22 mediates early host defense against attaching and effacing bacterial pathogens. Nat Med. 2008;14(3):282–9.
- Bouwhuis MA, Sweeney T, Mukhopadhya A, McDonnell MJ, O'Doherty JV. Maternal laminarin supplementation decreases Salmonella Typhimurium shedding and improves intestinal health in piglets following an experimental challenge with S Typhimurium post-weaning. Anim Feed Sci Technol. 2017;223:156–68. https://doi.org/10.1016/j.anifeedsci.2016.
- 39. Venardou B, O'Doherty JV, Maher S, Ryan MT, Gath V, Ravindran R, et al. Potential of a fucoidan-rich Ascophyllum nodosum extract to reduce Salmonella shedding and improve gastrointestinal health in weaned pigs naturally infected with Salmonella. J Anim Sci Biotechnol. 2022;13(1):39.
- Walsh AM, Sweeney T, O'Shea CJ, Doyle DN, O'Doherty JV. Effect of dietary laminarin and fucoidan on selected microbiota, intestinal morphology and immune status of the newly weaned pig. Br J Nutr. 2013;110(9):1630–8.
- 41. Vetvicka V, Vannucci L, Sima P. The effects of β-glucan on pig growth and immunity. Open Biochem J. 2014;1(1):89–93.

Publisher's Note

Springer Nature remains neutral with regard to jurisdictional claims in published maps and institutional affiliations.